Journal of Energy & Environment 1 (1999) 51-62

Development of Design Curves for the Double-Pass Photovoltaic Thermal Solar Collector

**K. Sopian, **H. T. Liu, **S. Kakac & **T. N. Veziroglu

*Department of Mechanical and Materials Engineering, 43600 Universiti Kebangsaan Malaysia Bangi, Selangor, Malaysia

**Dorgan Solar Laboratory, University of Miami, Coral Gables, USA

Abstract

Photovoltaic thermal collector is a combination of thermal and photovoltaic systems. It generates both thermal and electrical energies simultaneously. A theoretical model of a double-pass photovoltaic thermal solar collector was developed. An experimental setup of the collector was designed and fabricated to study the performance and to validate the model over a range of design condition such as mass flow rate and channel depth and operating condition such as ambient, inlet, and outlet temperatures and global solar radiation. Several important relationships between the design and operating conditions were obtained. These relationships affect the performance of the double-pass photovoltaic thermal solar collector. Hence, design curves for the photovoltaic thermal solar collector were developed. The designer would be able to predict the performance of the system using these design curves by selecting the required conditions. This include the effect of change in the channel depth, air mass flow rate global solar radiation, and the temperature rise of the collector on the thermal, photovoltaic and combined thermal photovoltaic efficiencies.

Nomenclature

A_c	Collector area, m^2
C_p	Specific heat of air, kJ/kg °C
d_1	Depth for the upper channel, cm
d_2	Depth for the lower channel, cm
T_{ref}	Reference temperature, 25 °C
h_{cgw}	Convective heat transfer between glass cover and wind (W/m^2 °C)
h_{cf1g}	Convective heat transfer between glass cover and upper channel air flow (W/m^2 °C)
h_{cf1pv}	Convective heat transfer between photovoltaic panel and upper channel air flow
h_{cf2pr}	Convective heat transfer between photovoltaic panel and lower channel air flow
h_{cf2pr}	Convective heat transfer between back-plate and upper channel air flow (W/m^2 °C)
h_{rpvg}	Radiative heat transfer between glass cover and photovoltaic panel (W/m^2 °C)
h_{rpvpr}	Radiative heat transfer between back-plate and photovoltaic panel (W/m^2 °C)
m	Mass flow rate, kg/s
P	Packing factor or fraction or area covered by photovoltaic cell
S	Solar radiation (W/m^2)
T_a	Ambient temperature (° C)
T_g	Glass temperature (° C)
T_{pv}	Photovoltaic panel temperature (° C)
T_{pr}	Back-plate temperature (° C)
T_s	Sky temperature ($T_a - 6$) (° C)
T_{f1}	Upper channel air temperature (° C)
T_{f2}	Lower channel air temperature (° C)
T_o	Outlet temperature, °C

T_i Inlet temperature, °C
U_t Overall loss coefficient from back of the system (W/m^2 °C)
W_{pv} Electric power generated by the photovoltaic panel (W)
η_{PVT} Combined photovoltaic thermal efficiency, %
η_{PV} Photovoltaic thermal efficiency, %
η_{ref} Photovoltaic reference efficiency at t 25 °C, %
η_{th} Thermal efficiency, %
α_g α_{pv} Absorptance of the glass cover and photovoltaic cells
α_1, α_2, β_1, β_2, C_1, C_2 Constants obtained by algebraic manipulations
γ Temperature correction factor
τ_g Transmittance of the glass cover

Introduction

Solar energy is the world's most abundant permanent source of energy. It is also an important and environmentally compatible source of renewable energy. The uses of non-renewable fuels, such as fossil fuels have many disadvantages also. Their combustion products produce pollution, acid rain and global warming. Use of clean energy sources such as solar energy would enable the world to improve the quality of life throughout the planet Earth, not only for humans, but also for its flora and fauna as well. So, there is a need to develop an ingenious method of solar energy conversion systems and then to substitute it where applications of fossil fuels are most vulnerable. One of the ingenious methods of solar energy conversion systems is the photovoltaic thermal solar collector system, which converts solar radiation directly to both thermal and electrical energies. In its simplest form, a photovoltaic thermal collector consists of photovoltaic cells affixed to the absorber surface of a flat-plate collector. The manufacturing, marketing, installation and space-saving advantages of obtaining two forms of energy from a single physical unit must be weighed against the reduced electrical and thermal performance of the photovoltaic thermal collector in comparison to separate photovoltaic and thermal collectors. However, potential advantages exist in combining photovoltaic cells with a thermal collector. Conceivably, the photovoltaic thermal collector cost would be less than the combined cost of separate collectors providing the same power. When integrated into a residential heating, cooling and electrical power system, the photovoltaic thermal collectors require about 50% less area than separate collectors that provide similar quantities of thermal and electric power [1]. Hence, these are important factors in the large retrofit residential market.

One of the early application of the photovoltaic thermal air heaters was at the residential scale experimental solar house at the Institute of Energy Conversion, the University of Delaware [2]. The collector is basically a single-pass system. The cover of the collector is made from abcite-coated plexiglass. The collector consists of two air channels. The first channel is a "static" channel between the cover and photovoltaic panel. The second channel is a bottom flow channel between the photovoltaic panel and back-plate for heat transfer. Hendrie [1] performed experimental analysis on a single-pass photovoltaic thermal air collector which consists of two glass covers with photovoltaic cells mounted on the underside of the inner glass cover. The inner glass cover acted as the primary absorber of incident solar radiation. A black-painted aluminum thermal absorber plate placed below the air flow channel receives solar radiation passing between the photovoltaic cells. For a solar radiation of 1000 W/m^2, ambient temperature of 22°C and average fluid temperature $(T_o+T_i)/2$ variations from 0 to 50°C, the cell efficiencies varied from 5.8 to 6.8%. In addition, the thermal efficiencies varied from 20 to 34% as the values of $(T_i - T_a)/S$ varied from 0 to 0.06°C m^2/W.

Researchers at the Brown University Photovoltaic Research Group installed twenty (2 ft by 6 ft) photovoltaic thermal air collectors on the roof of a residential (1200 square foot) building on the Brown University campus

[3]. The collector absorber surfaces were covered by 143 series connected 4 inch diameter commercial silicon photovoltaic cells. The nominal efficiency of the cells was 11% at a temperature of 25°C. Aluminum fins were bonded to the underside of each photovoltaic cells to enhance the heat transfer between the cells and the air flowing under it. The length of the fins was set at 1 inch to reduce the fan power. An entrance manifold directs the air into the bottom of pairs of photovoltaic thermal air heaters that were in series for the air flow. An exit manifold collects the air after its passage through the twenty air heaters and directs it through a heat exchanger for heating hot water into the building for space heating. The system also runs an electrically operated air-to-air heat pump, and a synchronous inverter. Typical power generated was 1.29kW at a solar radiation of 910 W/m^2.

Other studies published on photovoltaic thermal air collectors were conducted at the Indian Institute of Technology, Delhi [4, 5, and 6]. The design includes an air collector with air low passage between two metallic plates. The upper metallic plate was painted black and the photovoltaic cells were pasted over it. The material used to paste the cells on the absorber plate should be a thermal conductor but also an electrical insulator (this material is also known as pottant). A combination of an air collector and photovoltaic system parameters such as channel depth, length of collectors and mass flow rate were used by Bhargava *et al* [4] to compute the optimum area of the photovoltaic cells necessary to generate sufficient electricity for the fan. It was shown that the system was self sufficient only for certain design parameters. For instance, for self sufficiency, the channel depth should be 10 cm or more.

Sopian *et al* [7] and Choudhary and Garg [8] have studied theoretically the double-pass photovoltaic thermal solar collector. The double-pass systems produced more heat while simultaneously having a productive cooling effect on the photovoltaic cells. The use of the double-pass system resulted in an increase in pressure drop across the collector. However, the increase in the operating cost due to the increased pressure drop in the collector is considered small. This is due to the fact that the pressure drop across the collector is small compared to the total pressure drop of the system [9, 10].

In this paper, a comprehensive model of the double-pass photovoltaic thermal solar collector has been developed. The experimental validation and the resulting design curves of the double-pass photovoltaic thermal air collector are presented.

Theoretical background

Fig. 1 shows the double-pass hybrid solar collector with the heat transfer coefficients. To simplify the analysis the energy balance equations at the glass cover, photovoltaic panel and working fluid (air) are written under the following assumptions: (i) capacity effects of the glass cover, photovoltaic panel and back-plate have been neglected, (ii) the temperatures of the glass cover and plates vary in the fluid flow direction (i.e. the x-direction), (iii) the side losses are negligible and leakage of air to or from the collector is negligible and (iv) ideal gas with constant specific heat. The energy balance equation at the glass cover is and the energy balance for the back-plate is

$$\alpha_g S = h_{rgs}\left(T_g - T_s\right) + h_{cgw}\left(T_g - T_a\right) + h_{rpvg}\left(T_g - T_{pv}\right) + h_{cf1g}\left(T_g - T_{f1}\right) \tag{1}$$

The energy balance for the first air flow the equation is

$$\frac{mC_p}{d_1}\frac{dT_{f1}}{dx} = h_{cf1g}\left(T_g - T_{f1}\right) + h_{cpvf1}\left(T_{pv} - T_{f1}\right) \tag{2}$$

The second air flow energy balance equation in the lower channel and the is

$$-\frac{mC_p}{d_2}\frac{dT_{f2}}{dx} = h_{cpvf2}\left(T_{pv} - T_{f2}\right) + h_{cprf2}\left(T_{pr} - T_{f2}\right) \tag{3}$$

The energy balance on the photovoltaic panel is

$$\tau_g S\alpha_{pv}(1-P)+\tau_g S\alpha_{pv}P(1-\eta_{pv})-h_{rpvpr}(T_{pv}-T_{f2})-h_{rpvg}(T_{pv}-T_g)$$
$$-h_{cpvf1}(T_{pv}-T_{f1})-h_{cpvf2}(T_{pv}-T_{f2})=0 \quad (4)$$

$$h_{rpvpr}(T_{pv}-T_{pr})+h_{cprf2}(T_{f2}-T_{pr})=U_t(T_{pr}-T_a) \quad (5)$$

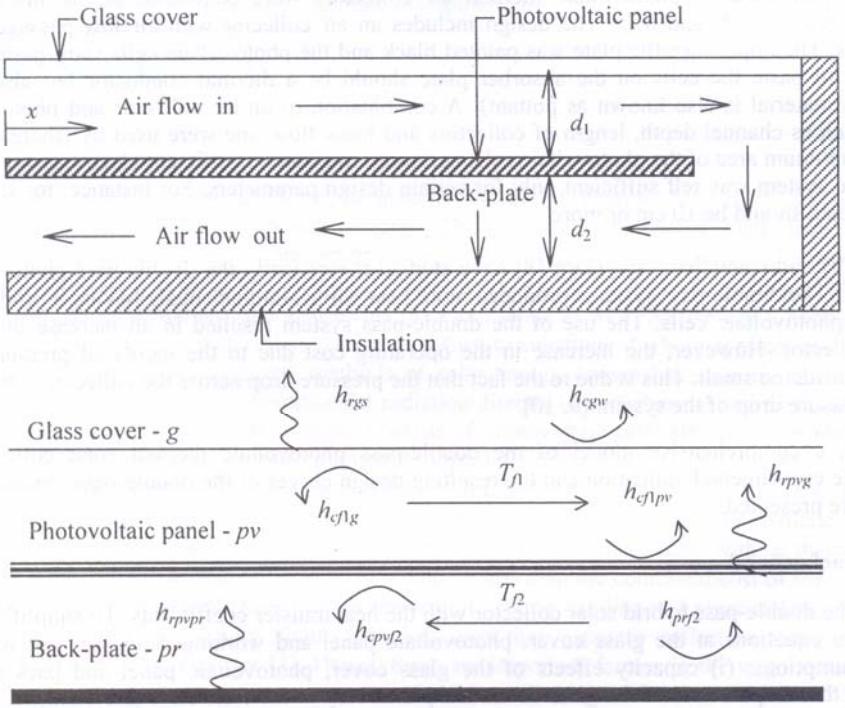

Fig. 1 Schematics of the double-pass photovoltaic thermal solar collector with heat transfer coefficients

Equations (1) through (5) can be combined to give the following two differential equations

$$\frac{dT_{f1}}{dx}=\alpha_1 T_{f1}+\alpha_2 T_{f2}+C_1 \quad (6)$$

$$\frac{dT_{f2}}{dx}=\beta_1 T_{f1}+\beta_2 T_{f2}+C_2 \quad (7)$$

The boundary conditions are as follows

$$T_{f1}(x=0)=T_i \qquad T_{f1}(x=L)=T_{f2}(x=L) \quad (8)$$

Hence, the outlet temperature T_{f2} ($x = L$) = T_o can be determined. The heat transfer coefficients used and the procedures of solving the above can be obtained from Sopian *et al.*, [7].

Experimental system

The schematic diagram of the experimental setup is shown in Fig. 2. The basic components are as follows: (i) the double-pass hybrid solar collector (ii) the support structure (iii) the air flow measurement system (iv) the temperature measurement system (vi) the solar radiation measurement system, and (vii) the data acquisition system. The photovoltaic panel has a width of 660 mm and a length of 1,476 mm. It consists of 36 silicon photovoltaic cells connected in series. The surface area of a single cell is 23.63 x 10^{-3} m^2. The total area of the panel covered by photovoltaic cells is 0.8505 m^2. Therefore, the packing factor P, or the fraction of the area of the absorber surface covered by the photovoltaic panel is 0.87. The efficiency of the photovoltaic panel is 14% at a mean panel temperature of 25°C. At 1000 W/m^2 and a panel temperature of 25°C, the rated power is 120 Watts. The maximum power voltage and current are 16.9 Volts and 7.1 Amperes respectively. In addition, at 1000 W/m^2 and a panel temperature of 60 °C, the maximum power voltage and current is 11.0 Volts and 7.6 Amperes respectively. Hence, the rated power is 83.6 Watts. The air flow system consists of the (i) inlet and outlet manifold, (ii) the flexible ducting system, (iii) fan and (iv) the mass flow rate measuring system. The height can be adjusted according to the position of the photovoltaic panel. The fan has a rated motor power of 1 / 30 hp and the speed is 3020 R P M.

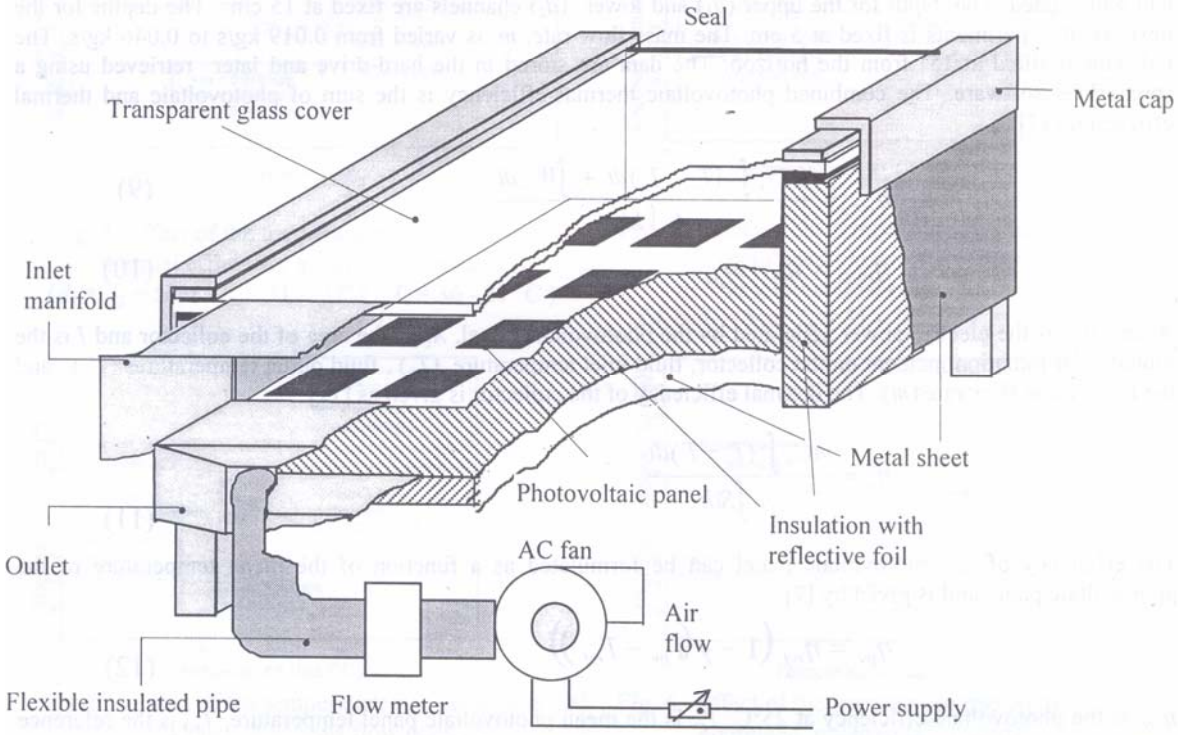

Fig. 2. The experimental setup of the double-pass photovoltaic thermal collector

The air flow sensing element is of the vane type probe head. The ambient temperature thermocouple is located outside in a well-ventilated location about 1.25 meter above the ground. Two thermocouples of type E are used for measuring the inlet temperature and placed at the beginning of the photovoltaic panel. The temperatures at the end of the first stream are measured by two thermocouples. Moreover, the outlet temperatures are measured by three thermocouples. Forty thermocouples of type E are used for determining the mean photovoltaic panel temperature and temperature distributions of the glass cover, photovoltaic panel, and the back-plate. The global

solar radiation is measured using a pyranometer. The pyranometer is mounted on the surface parallel to the collector surface in such a manner that it does not cast a shadow onto the collector plate. The main component of the data acquisition system for the experimental setup consists of the following (i) the personal computer, (ii) the data acquisition card, and (iii) the personal computer application program. The air flow meter has a resolution of 0.01 m/s and the accuracy of the probe is ±1 %. The error of the global solar radiation measurement is ± 1%. The error for temperature measurements is ± 0.1 °C.

Experimental procedures

It is difficult to obtain steady global solar radiation levels due to frequent movements of the cloud. The photovoltaic thermal solar collector has been operated at varying ambient temperature, air flow rate, channel depth, and global solar radiation conditions. Air is circulated for thirty minutes prior to the period in which data are taken. Data are sampled and averaged for a time period specified by the user using the application program of the data acquisition system. Data include global solar radiation, temperatures (inlet, end of the first pass, outlet, ambient, cover (top and bottom), photovoltaic panel (top and bottom), and back-plate), mass flow rate, and wind speed. The depth for the upper (d_1) and lower (d_2) channels are fixed at 15 cm. The depths for the next set of experiments is fixed at 5 cm. The mass flow rate, m, is varied from 0.019 kg/s to 0.046 kg/s. The collector is tilted at 15° from the horizon. The data are stored in the hard-drive and later retrieved using a spreadsheet software. The combined photovoltaic thermal efficiency is the sum of photovoltaic and thermal efficiencies [7]

$$\eta_{PVT} = \frac{mC_p \int (T_o - T_i)dt + \int W_{pv} dt}{A_c \int I dt} \tag{9}$$

$$\eta_{PVT} = \eta_{th} + \eta_{pv} \tag{10}$$

Where W_{pv} is the electric power generated by the photovoltaic panel, A_c is the area of the collector and I is the global solar radiation incident on the collector, fluid inlet temperature (T_i), fluid outlet temperatures (T_o), and the fluid mass flow rate (m). The thermal efficiency of the collector is given as [11]

$$\eta_{th} = \frac{mC_p \int (T_o - T_i)dt}{A_c \int S dt} \tag{11}$$

The efficiency of the photovoltaic panel can be formulated as a function of the mean temperature of the photovoltaic panel and is given by [7]

$$\eta_{pv} = \eta_{ref}\left(1 - \gamma\left(T_{pv} - T_{ref}\right)\right) \tag{12}$$

η_{Tref} is the photovoltaic efficiency at 25°C, T_{pv} is the mean photovoltaic panel temperature, T_{ref} is the reference temperature at 25°C, and γ is the temperature correction factor (0.0054/°C).

Results and observations

The primary parameters that influence the performance of the photovoltaic thermal solar collector have been identified as follows: (i) mean photovoltaic panel temperature (ii) mass flow rate (iii) upper and lower channels spacing (iv) ambient temperature (v) global solar radiation level (vi) photovoltaic panel length and (vii) packing factor (i.e. the fraction of the photovoltaic panel surface covered by photovoltaic cells). Two of the above parameters namely the photovoltaic panel length and the packing factor have been kept constant. The

experimental data have been thoroughly analyzed and manipulated in order to illustrate the relationships that exist between the design conditions such as channel depth and mass flow rate and the operating conditions such as ambient, inlet and outlet temperatures and global solar radiation. The design and operating conditions can be used to develop design curves for the system. Theoretical results are shown in full lines. The experimental results are compared and close agreements and trends have been obtained. The design curves include the followings (i) the effect of temperature rise on the efficiencies (thermal, photovoltaic and combined photovoltaic thermal efficiencies) (ii) effect of the global solar radiation on the temperature rise (iii) the effect of mass flow rate on the efficiencies (iv) the effect of the global solar radiation on efficiencies. Hence, the designer will be able to predict the performance of the double-pass photovoltaic thermal solar collector.

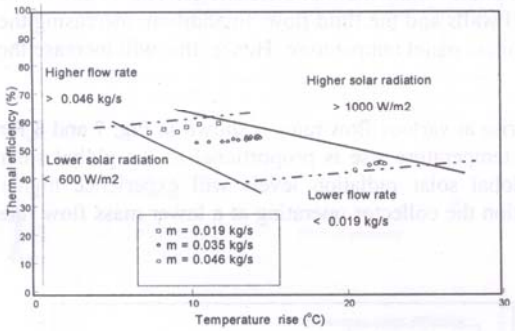

Fig. 3. Effect of the temperature rise on the thermal efficiency at various flow rates ($d_1 = d_2 = 5$cm $T_a = 31 - 32^\circ$ C $T_i = 36 - 37^\circ$ C)

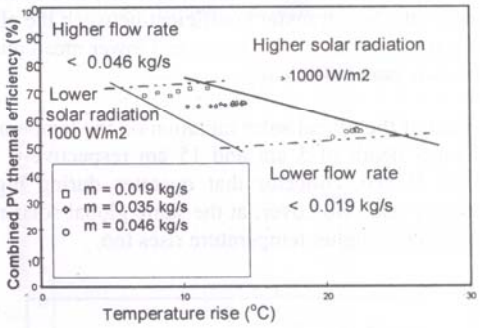

Fig. 4. Effect of the temperature rise on the combined photovoltaic thermal efficiency at various flow rates ($d_1 = d_2 = 5$cm $T_a = 31 - 32^\circ$ C $T_i = 36 - 37^\circ$ C)

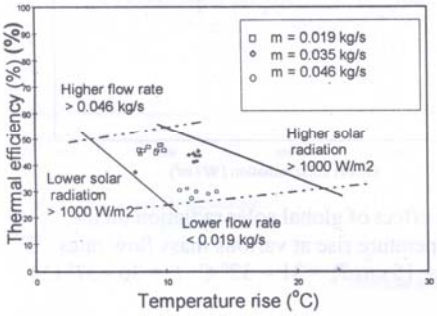

Fig. 5, Effect of the temperature rise on the thermal Efficiency at various flow rates ($d_1 = d_2 = 15$cm $T_a = 31 - 32^\circ$ C $T_i = 36 - 37^\circ$ C)

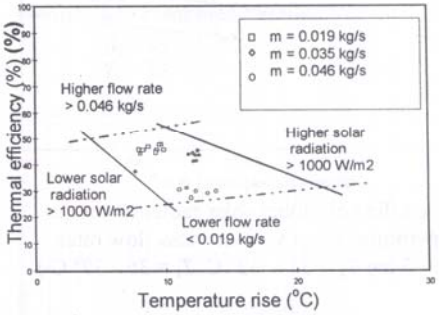

Fig. 6. Effect of the temperature rise on the combined photovoltaic thermal efficiency at various flow rates ($d_1 = d_2 = 15$cm $T_a = 31 - 32^\circ$ C $T_i = 36 - 37^\circ$ C)

The effect of the temperature rise on the thermal and combined photovoltaic thermal efficiencies can be seen in Fig. 3 through 6. The Fig. also show the region in which the experiments have been conducted with four lines that indicate the limits for the mass flow rate and global solar radiation. One of the lines shows the limit for mass flow rate that is less than 0.019 kg/s. The other line indicates the limit for mass flow rate greater than 0.046 kg/s. Also shown in the fig. are the limit lines for the global solar radiation. Therefore, the other two lines

indicate values for global solar radiation less than 600 W/m^2 and for global solar radiation greater than 1000 W/m^2.

Fig. 3 and 4 show the effect of the temperature rise on the thermal and the combined photovoltaic thermal efficiencies at various flow rates for the upper and lower channel depth of 5 cm. Fig. 5 and 6 sow these effects for the upper and lower channel depth of 15 cm. Hence, for a specific mass flow rate and global solar radiation levels the combinations of temperature rise, thermal, and combined photovoltaic thermal efficiencies can be obtained.

It can be seen from Fig. 3 through 6 that decreasing the flow channel height for the same mass flow rate results in an increased in the photovoltaic, thermal, and combined photovoltaic thermal efficiencies. This is due to the increase in the heat transfer coefficient between the channel walls and the fluid flow. In addition, increasing the heat transfer coefficient will result in a lower mean photovoltaic panel temperature. Hence, this will increase the photovoltaic panel efficiency.

The effect of the global solar radiation on the temperature rise at various flow rates is shown in Fig. 7 and 8 for the channel depth of 5 cm and 15 cm respectively. The temperature rise is proportional to the global solar radiation. Hence, collector that operates during high global solar radiation levels will experience higher temperature rise. Moreover, at the same global solar radiation the collector operating at a lower mass flow rate will experience higher temperature rises too.

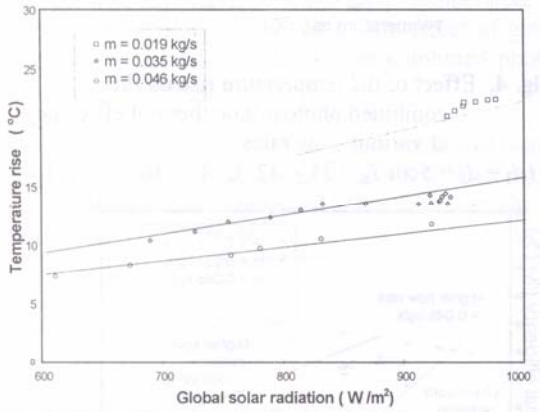

Fig. 7. The effect of global solar radiation on the temperature rise at various mass flow rates ($d_1 = d_2 = 5$ cm $T_a = 31 - 32^\circ$ C $T_i = 36 - 37^\circ$ C)

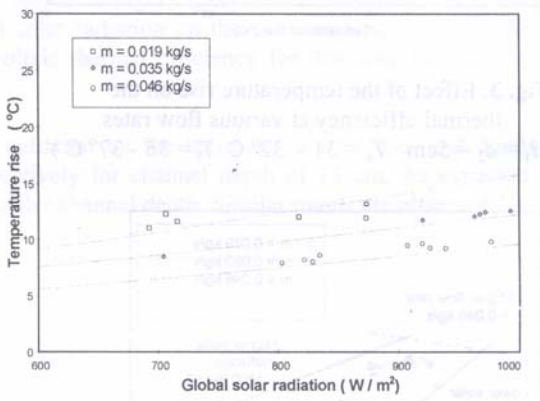

Fig. 8. The effect of global solar radiation on the temperature rise at various mass flow rates ($d_1 = d_2 = 15$ cm $T_a = 31 - 32^\circ$ C $T_i = 36 - 37^\circ$ C)

Hence, in these figures if the mass flow rate and global solar radiation are known then the temperature rise of the collector can be determined. It can also be observed in Fig. 8, that the slope of the theoretical lines for the lower flow rate is higher compared to the slope at higher flow rate. In other words, at lower mass flow rates the increase in temperature rise for every increase in the global solar radiation is more than for the higher flow rates. Comparison of Fig. 7 and 8 also show that the increases in temperature rise for all the three flow rates are lower than the one with a smaller channel depth. This is due to the decrease in heat transfer between the photovoltaic panel and fluid flow in the channels with larger depth. Moreover, for a given mass flow rate, the velocity of fluid is much lower in the collector in the larger channel depth.

Fig. 9, and 10 show the effect mass flow rate on the photovoltaic, thermal, and combined photovoltaic thermal efficiencies for the case where the channel depth are fixed at 5 cm and operating at a global solar radiation between 800 and 1000 W/m^2. Fig. 11 shows the effect of mass flow rates on the efficiencies for channel depth of 15 cm. The range of global solar radiation is between 600 to 1000 W/m^2. Therefore, cooling of the photovoltaic cells by increasing the mass flow rate will improve the combined photovoltaic thermal efficiency.

Fig. 12 through 14 show the effect of global solar radiation on the thermal, photovoltaic, and combined photovoltaic thermal efficiencies respectively at channel depth of 5 cm and flow rates of 0.019, 0.035, and 0.046 kg/s. From Fig. 12, as the mass flow rate increases the thermal efficiency will also increase. At mass flow rate of 0.019 kg/s, the thermal efficiency at 600 W/m^2 is lower than the thermal efficiency at 1000 W/m^2. Fig. 13 shows the effect of the global solar radiation on the photovoltaic efficiency at different mass flow rates.

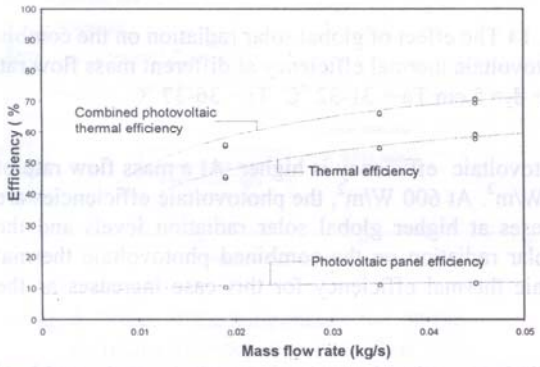

Fig. 9. The effect of mass flow rate on the photovoltaic, thermal and combined photovoltaic thermal efficiencies ($d_1 = d_2 = 5$ cm $T_a = 31$ - 32° C $T_i = 36$ - 37° C $S = 1000$ W/m^2)

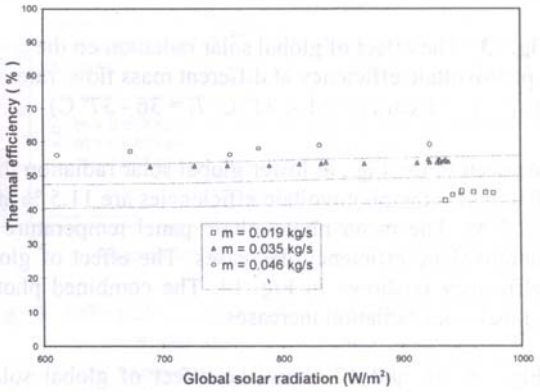

Fig. 10. The effect of mass flow rate on the hotovoltaic, thermal, and combined photovoltaic therma efficiencies ($d_1 = d_2 = 5$ cm $T_a = 31$ - 32° C $T_i = 36$ - 37° C $S = 800$ W/m^2)

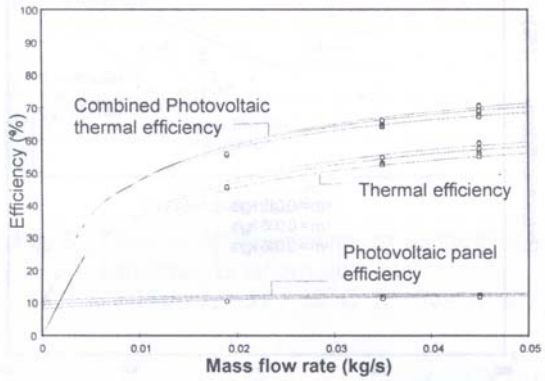

Fig. 11. The effect of mass flow rate on the photovoltaic, thermal, and combined photovoltaic thermal efficiencies ($d_1 = d_2 = 15$ cm $T_a = 31$ - 32° C $T_i = 36$ - 37° C $S = 600 - 1000$ W/m^2)

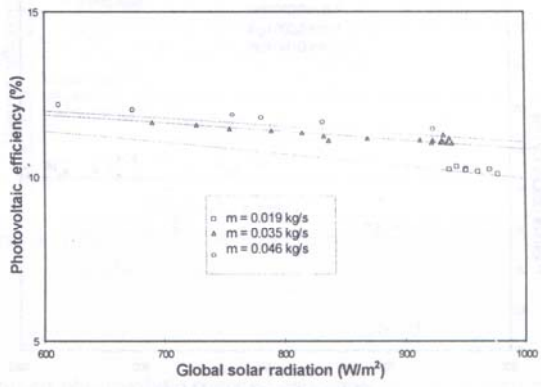

Fig. 12. The effect of global solar radiation on the thermal efficiency at different mass flow rates ($d_1 = d_2 = 5$ cm $T_a = 31$ - 32° C $T_i = 36$ - 37° C)

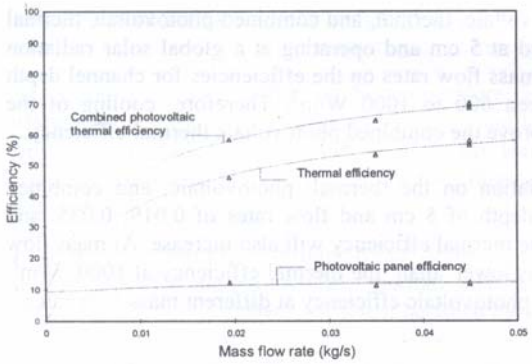

Fig. 13. The effect of global solar radiation on the photovoltaic efficiency at different mass flow rates ($d_1 = d_2 = 5$ cm $T_a = 31 - 32^\circ$ C $T_i = 36 - 37^\circ$ C)

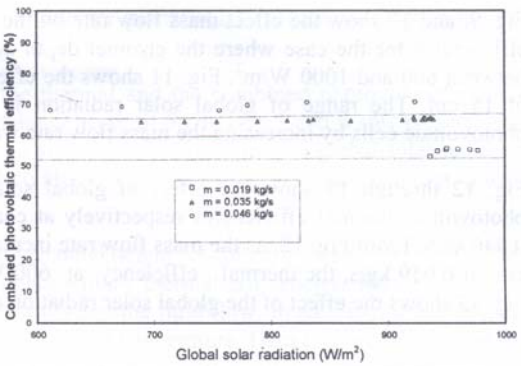

Fig. 14 The effect of global solar radiation on the combined photovoltaic thermal efficiency at different mass flow rates ($d_1 = d_2 = 5$ cm Ta = 31-32 °C Ti = 36-37 °C

As seen in the Fig., at lower global solar radiation the photovoltaic efficiency is higher. At a mass flow rate of 0.046 kg/s the photovoltaic efficiencies are 11.5 % at 900 W/m^2. At 600 W/m^2, the photovoltaic efficiencies are 12.2 %. The mean photovoltaic panel temperature increases at higher global solar radiation levels and the photovoltaic efficiency decreases. The effect of global solar radiation on the combined photovoltaic thermal efficiency is shown in Fig. 14. The combined photovoltaic thermal efficiency for this case increases as the global solar radiation increases.

Fig. 15, 16 and 17 show the effect of global solar radiation on the thermal, photovoltaic, and combined photovoltaic thermal efficiencies of the collector respectively for channel depth of 15 cm. As expected, the efficiencies are lower compared to the collector with smaller channel depth. Similar trends are observed for the effects on efficiencies.

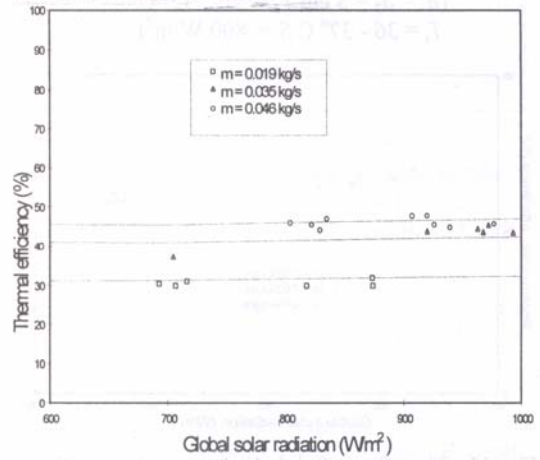

Fig. 15. The effect of global solar radiation on the thermal efficiency at different mass flow rates ($d_1 = d_2 = 15$ cm $T_a = 31 - 32^\circ$C $T_i = 36 - 37^\circ$C)

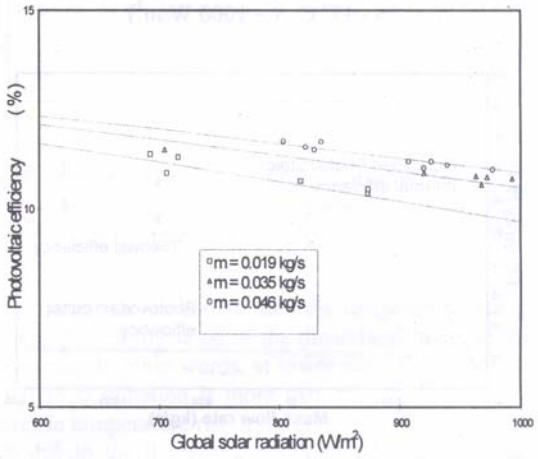

Fig. 16. The effect of global solar radiation on the photovoltaic efficiency at different mass flow rates ($d_1 = d_2 = 15$ cm $T_a = 31 - 32^\circ$C $T_i = 36 - 37^\circ$C)

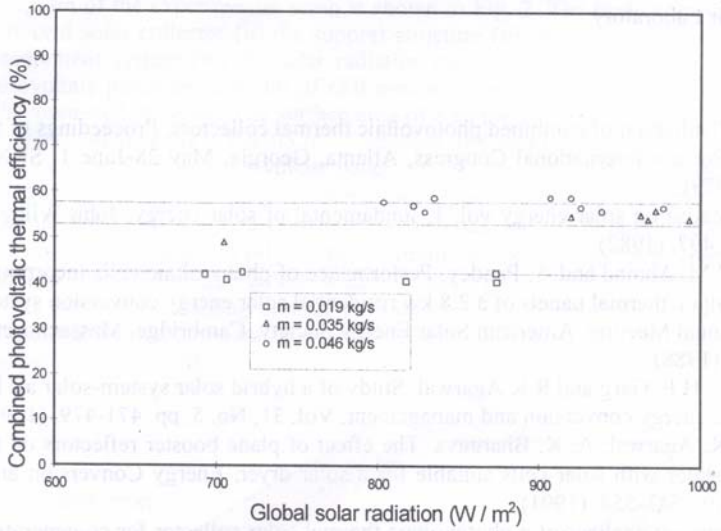

Fig. 17. The effect of global solar radiation on the combined photovoltaic thermal efficiency at different mass flow rates ($d_1 = d_2 = 15$ cm $T_a = 31$ - 32^oC $T_i = 36$ - 37^oC)

Conclusions

A mathematical model of a double-pass photovoltaic thermal solar collector has been developed. An experimental double-pass photovoltaic thermal hybrid solar collector has been designed, fabricated, and tested. Design curves showing variations in the design and operating conditions are developed. The curves would be useful to the designer to observe the effect of temperature rise on the efficiencies, and the effect of the global solar radiation on temperature rise, and the efficiencies, the effect of mass flow rate on the efficiencies. The double-pass photovoltaic thermal solar collector can produce more heat than that of the conventional single-pass system. In addition it has better productive cooling effect on the photovoltaic cells. The main advantages of the photovoltaic thermal collectors are : (a) by cooling the photovoltaic cells and maintaining (limiting) certain operating temperatures, higher performance of the photovoltaic cells are obtained, (b) the heat, dissipated otherwise to the surrounding atmosphere can be collected as thermal energy, (d) a decrease in the produced energy costs due to a lower packaging cost and better use of energy conversion process. This type of collector is attractive for solar application in which limited space and area-related installation cost are of primary concern, and the space needed to install side-by-side solar thermal and photovoltaic collectors is not readily available. Recent advances in the production methods of photovoltaic cells will reduce their initial cost and increase the demand for the application of photovoltaic systems. Under such economically favorable conditions, the use of photovoltaic thermal hybrid solar collector would be ideal for a wide variety of applications.

Acknowledgements - This project was financed by the Dorgan Solar Laboratory, University of Miami at Coral Gables. K. Sopian would like to thank the Universiti Kebangsaan Malaysia for financial support during his work at the Dorgan Solar Laboratory.

References

[1] Hendrie, S.D. Evaluation of combined photovoltaic thermal collectors, Proceedings of the International Solar Energy Society International Congress, Atlanta, Georgia, May 28-June 1, SUN II, Vol. 3, pp. 1865-1869, (1979).

[2] Garg, H.P., Treatise on solar energy vol. 1, fundamental of solar energy, John Wiley and Sons, New York, Ch. 6, p. 497, (1982)

[3] Loferski, J.J., J.M. Ahmad and A. Pandey, Performance of photovoltaic cells incorporated into unique hybrid photovoltaic/thermal panels of a 2.8 kw residential solar energy conversion system, Proceedings of the 1988 Annual Meeting, American Solar Energy Society, Cambridge, Massachusetts, June 20 –24, pp. 427 – 432, (1988).

[4] Bhargava, A.K., H.P. Garg and R.K Agarwal, Study of a hybrid solar system-solar air heater combined with solar cells, energy conversion and management, Vol. 31, No. 5, pp. 471-479, (1991).

[5] Garg, H.P., P.K. Agarwal, A. K. Bhargava, The effect of plane booster reflectors on the performance of a solar air heater with solar cells suitable for a solar dryer, Energy Conversion and Management, Vol. 32, No.6, pp. 543-554, (1991).

[6] Prakash, J., Transient analysis of a photovoltaic thermal solar collector for co-generation of electricity and hot air/water, energy conversion and management, Vol. 35, No. 11, pp. 967-972, (1994)

[7] Sopian, K., K. S. Yigit, H.T. Liu, S. Kakac, and T. N. Veziroglu, An investigation into the performance of a double-pass photovoltaic thermal solar collector, R. J. krane (ed) thermodynamics and design, analysis, and improvement of energy systems, ASME International Mechanical Engineering Congress and Exhibition, San Francisco, November 12-17, AES-Vol. 35, pp. 89-94, (1995).

[8] Choudhary C. and H. P. Garg, Performance of two pass photovoltaic/thermal air heater, Renewable Energy, 9 (1-4), 1803 –1806, (1996).

[9] Wijeysundera, N.E., L.L. An and L.E. Tyioe, Thermal performance study of two pass solar air heater, Solar Energy, Vol. 28, No. 5, pp. 363 – 370, (1982).

[10] Mohamad, A. A., High efficiency solar air heater, Solar Energy, 60, 2, 71-76, (1997)

[11] Duffie, J. A. and W. A. Beckman, Solar Engineering of Thermal Processes, Wiley Interscience, 2nd ed, New York, Ch. 7, pp. 351 – 354, (1991).